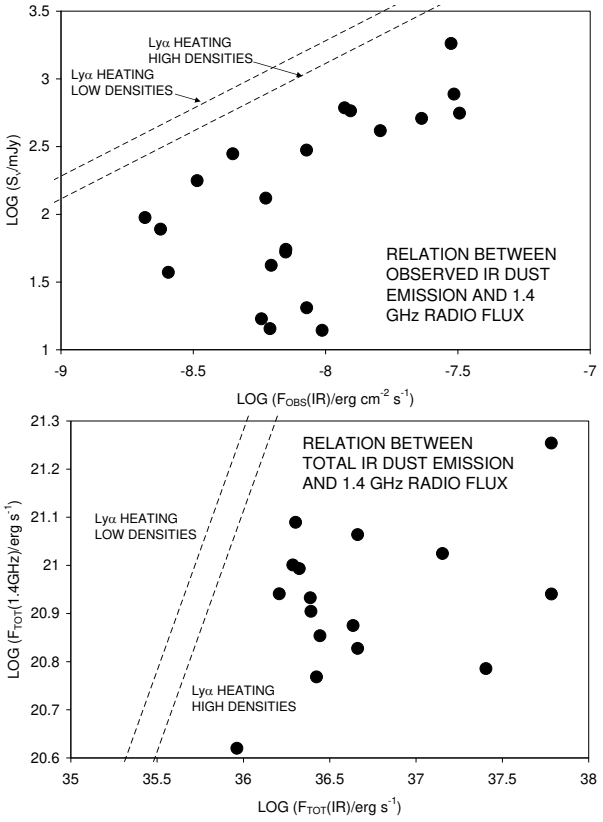

Fig. 9. A comparison between observed 1.4 GHz and integrated FIR fluxes (upper panel), and the intrinsic (distance corrected) counterparts of these fluxes (lower panel). The diagonal lines correspond to the trends where Lyα heating dominates the results, and represent low and high values of the nebular density. It is clear that Lyα heating represents ≤ 0.5 of the energy budget of the IR emitting grains.

is typical of the luminosities of PNe central stars, this suggests that a large fraction of the radiation is being absorbed by dust – a situation which would be consistent with the high levels of reddening observed in proto-planetary nebulae (PPNe).

It is finally interesting to adapt the analysis of Lyα heating of Pottasch et al. (1984) to the present AKARI results. The results of such a procedure are illustrated in Figure 9, where we show the relation between observed integrated IR and 1.4 GHz emission, and between intrinsic (distance corrected) IR and 1.4 GHz results (lower panel). The trends expected for Lyα heating are indicated by the dashed diagonal lines, determined for high and low density nebular regimes. It would appear that the infrared excess (IRE), corresponding to the ratio of the observed flux to Lyα heating, is of order > 2 for all of this present sample PNe. It is therefore clear that further heating of the grains is required over and above that expected by Lyα photons.

One would anticipate that values of the IRE would be largest where PNe are more compact, Lyα fluxes are smaller, and direct heating by the stellar radiation field is greatest. Subsequent nebular expansion would lead to further ionization of the shell; increased fluxes of Lyα photons; and the dilution of the stellar radiation field. Under these circumstances, the IRE would be expected to decline rather precipitously, and achieve minimum values of the order of unity.

To investigate whether some such evolution is actually occurring, we have determined FIR luminosities for a broad range of PNe. This involved using the 18 and 65 μm fluxes to determine $T_{\rm GR}$; assuming a grain emissivity exponent $\gamma = 1$; and employing 1.4 GHz fluxes to evaluate Lyα heating. We assume Lyα photon production rates relevant for lower density PNe, whilst the distances and sizes of the sources are taken from Tables 1 and 2. Under these circumstances, appropriate integration of the emission curves show that the luminosity of the source can be represented through

$$L = 3.11{\times}10^{13}\left[\frac{\mathrm{F}_\nu(90\ \mu m)}{\mathrm{Wm^{-2}Hz}}\right]\left[\frac{d}{\mathrm{kpc}}\right]^2\left[\sum_{i=0}^{4} a_i T_{\rm GR}^i\right]^{-1} L_\odot\,, \quad (1)$$

where d is source distance, the polynomial terms $[a_0, ..., a_4]$ are given by $[7.162 \times 10^{10}, -1.834 \times 10^9, 1.868{\times}10^7, -8.742{\times}10^4, 1.564{\times}10^2]$, and the expression is valid for temperatures $70 < T_{\rm GR}/\mathrm{K} < 160$. Similar expressions may be derived for differing values of γ.

Note that both here, and in the analysis of the results in Figure 5 (see above), we have used 90 μm fluxes to scale the results. This is advantageous for a variety of reasons. Not only are these results taken with the most sensitive of the FIS detectors –leading to larger numbers of PNe detections than in other channels– but this wavelength lies close to the continuum peak for most of the PNe SEDs. We have also assessed that levels of line contamination are likely to be modest (§ 3.1), although there is evidence that contaminants may be larger than is supposed (see § 3.2 and Figure 5). It is unlikely, however, that luminosities are very greatly in error, or that mean biases are greater than ∼0.1 dex.

The results of this analysis are illustrated in Figure 10, where the IRE is represented against nebular diameter. It is plain from this that some evolution does indeed appear to be occurring, with values of IRE approaching ∼50 for diameters < 0.07 pc. Al-